Hindawi Publishing Corporation
EURASIP Journal on Wireless Communications and Networking
Volume 2011, Article ID 849105, 10 pages
doi:10.1155/2011/849105

Research Article

Performance Analysis of Ad Hoc Dispersed Spectrum Cognitive Radio Networks over Fading Channels

Khalid A. Qaraqe,[1] Hasari Celebi,[1] Muneer Mohammad,[2] and Sabit Ekin[2]

[1] *Department of Electrical and Computer Engineering, Texas A&M University at Qatar, Education City, Doha 23874, Qatar*
[2] *Department of Electrical and Computer Engineering, Texas A&M University, College Station, TX 77843, USA*

Correspondence should be addressed to Hasari Celebi, hasari.celebi@qatar.tamu.edu

Received 1 September 2010; Revised 6 December 2010; Accepted 19 January 2011

Academic Editor: George Karagiannidis

Cognitive radio systems can utilize dispersed spectrum, and thus such approach is known as dispersed spectrum cognitive radio systems. In this paper, we first provide the performance analysis of such systems over fading channels. We derive the average symbol error probability of dispersed spectrum cognitive radio systems for two cases, where the channel for each frequency diversity band experiences independent and dependent Nakagami-m fading. In addition, the derivation is extended to include the effects of modulation type and order by considering M-ary phase-shift keying (M-PSK) and M-ary quadrature amplitude modulation (M-QAM) schemes. We then consider the deployment of such cognitive radio systems in an ad hoc fashion. We consider an ad hoc dispersed spectrum cognitive radio network, where the nodes are assumed to be distributed in three dimension (3D). We derive the effective transport capacity considering a cubic grid distribution. Numerical results are presented to verify the theoretical analysis and show the performance of such networks.

1. Introduction

Cognitive radio is a promising approach to develop intelligent and sophisticated communication systems [1, 2], which can require utilization of spectral resources dynamically. Cognitive radio systems that employ the dispersed spectrum utilization as spectrum access method are called dispersed spectrum cognitive radio systems [3]. Dispersed spectrum cognitive radio systems have capabilities to provide full frequency multiplexing and diversity due to their spectrum sensing and software defined radio features. In the case of multiplexing, information (or signal) is splitted into K data nonequal or equal streams and these data streams are transmitted over K available frequency bands. In the case of diversity, information (or signal) is replicated K times and each copy is transmitted over one of the available K bands as shown in Figure 1. Note that the frequency diversity feature of dispersed spectrum cognitive radio systems is only considered in this study.

Theoretical limits for the time delay estimation problem in dispersed spectrum cognitive radio systems are investigated in [3]. In this study, Cramer-Rao Lower Bounds (CRLBs) for known and unknown carrier frequency offset (CFO) are derived, and the effects of the number of available dispersed bands and modulation schemes on the CRLBs are investigated. In addition, the idea of dispersed spectrum cognitive radio is applied to ultra wide band (UWB) communications systems in [4]. Moreover, the performance comparison of whole and dispersed spectrum utilization methods for cognitive radio systems is studied in the context of time delay estimation in [5]. In [6, 7], a two-step time delay estimation method is proposed for dispersed spectrum cognitive radio systems. In the first step of the proposed method, a maximum likelihood (ML) estimator is used for each band in order to estimate unknown parameters in that band. In the second step, the estimates from the first step are combined using various diversity combining techniques to obtain final time delay

estimate. In these prior works, dispersed spectrum cognitive radio systems are investigated for localization and positioning applications. More importantly, it is assumed that all channels in such systems are assumed to be independent from each other. In addition, single path flat fading channels are assumed in the prior works. However, in practice, the channels are not single path flat fading, and they may not be independent each other. Another practical factor that can also affect the performance of dispersed spectrum cognitive radio networks is the topology of nodes. In this context, several studies in the literature have studied the use of location information in order to enhance the performance of cognitive radio networks [8, 9]. It is concluded that use of network topology information could bring significant benefits to cognitive radios and networks to reduce the maximum transmission power and the spectral impact of the topology [10]. In [11], the effect of nonuniform random node distributions on the throughput of medium access control (MAC) protocol is investigated through simulation without providing theoretical analysis. In [12], a 3D configuration-based method that provides smaller number of path and better energy efficiency is proposed. In [13], 2D and 3D structures for underwater sensor networks are proposed, where the main objective was to determine the minimum numbers of sensors and redundant sensor nodes for achieving communication coverage. In [14–16], the authors represent a new communication model, namely, the square configuration (2D), to reduce the internode interference (INI) and study the impact of different types of modulations over additive white gaussian noise (AWGN) and Rayleigh fading channels on the effective transport capacity. Moreover, it is assumed that the nodes are distributed based on square distribution (i.e., 2D). Notice that the effects of node distribution on the performance of dispersed spectrum cognitive radio networks have not been studied in the literature, which is another main focus of this paper.

In this paper, performance analysis of dispersed spectrum cognitive radio systems is carried out under practical considerations, which are modulation and coding, spectral resources, and node topology effects. In the first part of this paper, the performance analysis of dispersed spectrum cognitive radio systems is conducted in the context of communications applications, and average symbol error probability is used as the performance metric. Average symbol error probability is derived under two conditions, that is, the scenarios when each channel experiences independent and dependent Nakagami-m fading. The derivation for both cases is extended to include the effects of modulation type and order, namely, M-ary phase-shift keying (M-PSK) and M-ary quadrature amplitude modulation (M-QAM). The effects of convolutional coding on the average symbol error probability is also investigated through computer simulations. In the second part of the paper, the expression for the effective transport capacity of ad hoc dispersed spectrum cognitive radio networks is derived, and the effects of 3D node distribution on the effective transport capacity of ad hoc dispersed spectrum cognitive radio networks are studied through computer simulations [17].

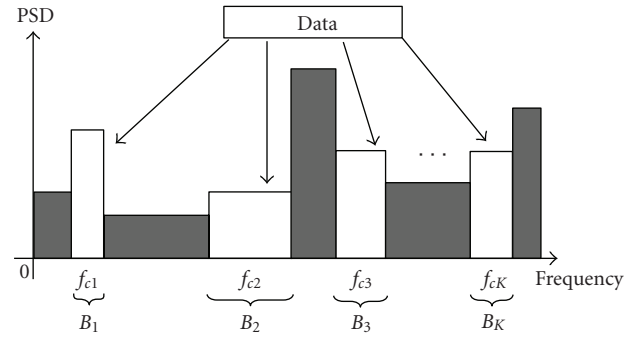

Figure 1: Illustration of dispersed spectrum utilization in cognitive radio systems. White and gray bands represent available and unavailable bands after spectrum sensing, respectively.

The paper is organized as follows. In Section 2, the system, spectrum, and channel models are presented. The average symbol error probability is derived considering different fading conditions and modulation schemes in Section 3. In Section 4, the analysis of the effective transport capacity for the 3D node distribution is provided. In Section 5, numerical results are presented. Finally, the conclusions are drawn in Section 6.

2. System, Spectrum, and Channel Models

The baseband system model for the dispersed spectrum cognitive radio systems is shown in Figure 2. In this model, opportunistic spectrum access is considered, where spectrum sensing and spectrum allocation (i.e., scheduling) are performed in order to determine the available bands and the bands that will be allocated to each user, respectively. Note that we assumed that these two processes are done prior to implementing dispersed spectrum utilization method. As a result, a single user that will use K bands simultaneously is considered in order to simplify the analysis in this study. The information of K is conveyed to the dispersed spectrum utilization system. In this stage, it is assumed that there are K available bands with identical bandwidths and dispersed spectrum utilization uses them. Afterwards, transmit signal is replicated K times in order to create frequency diversity. Each signal is transmitted over each fading channel and then each signal is independently corrupted by AWGN process. At the receiver side, all the signals received from different channels are combined using Maximum Ratio Combining (MRC) technique.

Since there is not any complete statistical or empirical spectrum utilization model reported in the literature, we consider the following spectrum utilization model. Theoretically, there are four random variables that can be used to model the spectrum utilization. These are the number of available band (K), carrier frequency (f_c), corresponding bandwidth (B), and power spectral density (PSD) or transmit power (P_{tx}) [18]. In the current study,

K is assumed to be deterministic. We also assume that PSD is constant and it is the same for all available bands, which results in a fixed SNR value. Additionally, since we consider baseband signal during analysis, the effect of f_c such as path loss are not incorporated into the analysis. Ergo, the only random variable is the bandwidth of the available bands which is assumed to be uniformly distributed [18] with the limits of $B_{\min}$ and $B_{\max}$, where $B_{\min}$ and $B_{\max}$ are the minimum and maximum available absolute bandwidths, respectively. In addition, we assume perfect synchronization in order to evaluate the performance of dispersed spectrum cognitive radio systems. The analysis of the system is given as follows.

The modulated signal with carrier frequency f_c is given by

$$s(t) = R\left\{\tilde{s}(t)e^{j2\pi f_c t}\right\}, \tag{1}$$

where $R\{\cdot\}$ denotes the real part of the argument, f_c is the carrier frequency, and $\tilde{s}(t)$ represents the equivalent low-pass waveform of the transmitted signal.

For $i = 1, 2, 3, \ldots. K$ dispersed bands in Figure 1, the modulated signal waveform of the ith band can be expressed as

$$s_i(t) = R\left\{\tilde{s}(t)e^{j2\pi f_{ci} t}\right\}, \tag{2}$$

where we assume that there is not carrier frequency offset in any frequency diversity branch. Note that the same modulated signal is transmitted over K dispersed bands in order to create frequency diversity. The channel for ith band is characterized by an equivalent low-pass impulse response, which is given by

$$h_i(t) = \sum_{l=1}^{L} \alpha_{i,l}\delta(t - \tau_{i,l})e^{-j\varphi_{i,l}}, \tag{3}$$

where $\alpha_{i,l}$, $\tau_{i,l}$, and $\varphi_{i,l}$ are the gain, delay, and phase of the lth path at ith band, respectively. Slow and nonselective Nakagami-m fading for each frequency diversity channel are assumed.

In the complex baseband model, the received signal for the ith band can be expressed as

$$r_i(t) = \sum_{l=1}^{L} \alpha_{i,l}s_i(t - \tau_{i,l})e^{-j\varphi_{i,l}} + n_i(t), \tag{4}$$

where $n_i(t)$ is the zero mean complex-valued white Gaussian noise process with power spectral density N_0. The SNR from each diversity band (γ_i) is combined to obtain the total SNR (γ_{Tot}), which is defined as

$$\gamma_{\text{Tot}} = \sum_{i=1}^{K} \gamma_i. \tag{5}$$

Notice from (5) that dispersed spectrum utilization method can provide full SNR adaptation by selecting required number of bands adaptively in the dispersed spectrum. This enables cognitive radio systems to support goal driven and autonomous operations.

The γ_{Tot} can be expanded to be written in the form of SNR of ith band with respect to the SNR of the first band. Hence, assume that the received power from the first band is equal to p and the AWGN experienced in this band has a power spectral density of N_0. Assume that the received power from the ith band is equal to $(\alpha_i p)$ and the AWGN experienced in this band has a power spectral density of $(\beta_i N_0)$. Thus, the total SNR can be expressed as

$$\gamma_{\text{Tot}} = \gamma_1 + \sum_{i=2}^{K} \kappa_i \gamma_1, \tag{6}$$

where $\gamma_1 = p/N_0$ and $\kappa_i = \alpha_i/\beta_i$. We assumed single-cell and single user case in this study. However, the analysis can be extended to multiple cells and multiuser cases, which is considered as a future work. At this point, we have obtained the total SNR, and in order to provide the performance analysis the average symbol error probability for two different cases, independent and dependent channels, are derived in the following section.

3. Average Symbol Error Probability

In this section, we derive the average symbol error probability expressions of dispersed spectrum cognitive radio systems for both independent and dependent fading channel cases considering M-PSK and M-QAM modulation schemes. We selected these two modulation schemes arbitrarily. However, the analysis can be extended to other modulation types easily.

3.1. Independent Channels Case. We assume Nakagami-m fading channel for each band. In order to derive the expression of the average symbol error probability (P_s) for both M-PSK and M-QAM modulations, we utilize the Moment Generator Function (MGF) approach. By using (6), the MGF of the dispersed spectrum cognitive radio systems over Nakagami-m channel is obtained, which is given by

$$\mu(s) = \left(1 - \frac{s\left(\gamma_{\text{Tot}}/\sum_{i=1}^{K}\kappa_i\right)(\kappa_i)}{m}\right)^{-m\kappa_i}, \tag{7}$$

where m is the fading parameter and $s = -g/\sin\phi^2$, in which g is a function of modulation order M. Therefore, for M-QAM and M-PSK modulation schemes, g is $g = 1.5/(M-1)$ and $g = \sin^2(\pi/M)$, respectively.

3.1.1. M-QAM. P_s for dispersed spectrum cognitive radio systems is obtained by averaging the symbol error probability

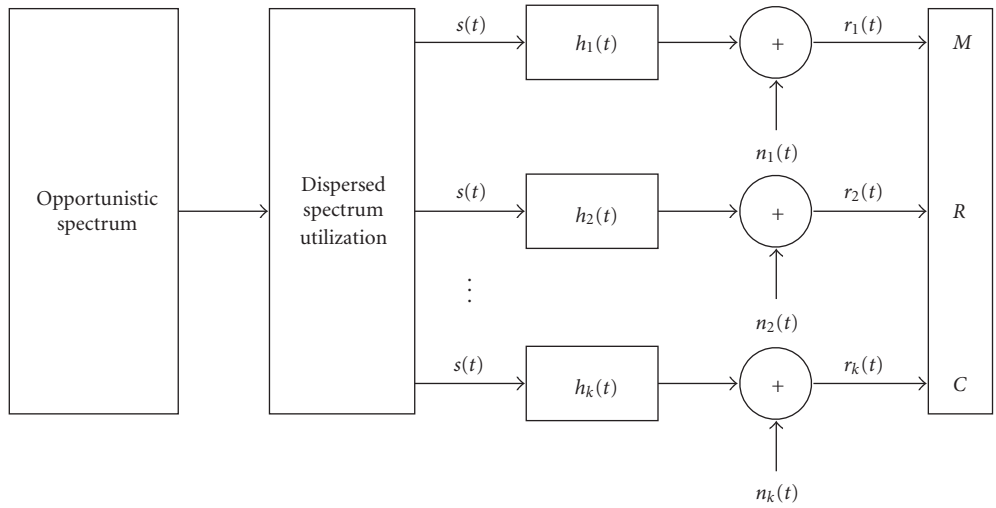

Figure 2: Baseband system model for dispersed spectrum cognitive radio systems.

$P_s(\gamma)$ over Nakagami-m fading distribution channel $P_{\gamma s}(\gamma)$, which is given by [19]

$$\begin{aligned} P_s &= \int_0^{\infty} P_s(\gamma) P_{\gamma s}(\gamma)\, d\gamma \\ &= \frac{4}{\pi}\left(\frac{\sqrt{M}-1}{\sqrt{M}}\right)\left[\int_0^{\pi/2} \mu(s)\, d\phi - \left(\frac{\sqrt{M}-1}{\sqrt{M}}\right)\int_0^{\pi/4} \mu(s)\, d\phi\right] \\ &= \frac{4}{\pi}\left(\frac{\sqrt{M}-1}{\sqrt{M}}\right) \\ &\quad \times \left[\int_0^{\pi/2}\left(1 - \frac{s(\gamma_{\mathrm{Tot}}/\sum_{i=1}^{K}\kappa_i)(\kappa_i)}{m}\right)^{-m\kappa_i} d\phi \right. \\ &\quad \left. - \left(\frac{\sqrt{M}-1}{\sqrt{M}}\right)\int_0^{\pi/4}\left(1 - \frac{s\left(\gamma_{\mathrm{Tot}}/\sum_{i=1}^{K}\kappa_i\right)(\kappa_i)}{m}\right)^{-m\kappa_i} d\phi\right]. \end{aligned} \tag{8}$$

3.1.2. M-PSK. By taking the same steps as in the M-QAM case, P_s for M-PSK is obtained as follows [19]:

$$P_s = \frac{1}{\pi}\int_o^{(M-1)(\pi/M)}\left(1 - \frac{s\left(\gamma_{\mathrm{Tot}}/\sum_{i=1}^{K}\kappa_i\right)(\kappa_i)}{m}\right)^{-m\kappa_i} d\phi. \tag{9}$$

3.2. Dependent Channels Case. To show the effects of dependent case in our system, we just need to use the covariance matrix that shows how the K bands are dependent. To the best of our knowledge, unfortunately there is not empirical model or study on the dependency of dispersed spectrum cognitive radio or frequency diversity of channels, and determining such covariance matrix requires an extensive measurement campaign. However, there are studies on the dependency of space diversity channels [20, 21]. Therefore, we use two arbitrary correlation matrices for the sake of conducting the analysis here. These two arbitrary correlation matrices are linear and triangular, and they are referred to as *Configuration A* and *Configuration B*, respectively, in the current study.

In our system, it is assumed that there are K correlated frequency diversity channels, each having Nakagami-m distribution. The basic idea is to express the SNR in terms of Gaussian distributions, since it is easy to deal with Gaussian distribution regardless of its complexity. The instantaneous SNR of parameter m_i for each band can be considered as the sum of squares of $2m_i$ independent Gaussian random variables which means that the covariance matrix of the total SNR can be expressed by $(2\sum_{i=1}^{K} m_i) \times (2\sum_{i=1}^{K} m_i)$ matrix with correlation coefficient between Gaussian random variables [22]. The MGF of Nakagami-m fading for the dependent case is defined as [23]

$$\mu(s) = \frac{1}{\prod_{n=1}^{N}(1 - 2s\xi_n)^{1/2}}, \tag{10}$$

where $s = -g/\sin^2\phi$, $N = 2\sum_{i=1}^{K} m_i$, and ξ_n are eigenvalues of covariance matrix for $n = 1, 2, \ldots N$.

The dimension of covariance matrix depends on N which means that there is always $N - K$ repeated eigenvalues with $2m_i - 1$ repeated eigenvalues per band. This is expected since the derivation depends on the facts that all the bands depend on each other. Thus, by using (10), the MGF for the dispersed spectrum cognitive radio systems in the case of dependent channels case can be expressed as

$$\mu(s) = \prod_{i=1}^{K}\left(1 - 2s(\gamma_i e_i)\right)^{-m_i}, \tag{11}$$

where e_i is the eigenvalue of covariance matrix for the ith band.

3.2.1. M-QAM. P_s for M-QAM modulation scheme is obtained using (8) and it is given by

$$P_s = \frac{4}{\pi}\left(\frac{\sqrt{M}-1}{\sqrt{M}}\right) \times \left[\int_0^{\pi/2}\left(\prod_{i=1}^{K}\left(1-2s(\gamma_i e_i)^{-m_i}\right)\right)d\phi - \left(\frac{\sqrt{M}-1}{\sqrt{M}}\right)\int_0^{\pi/4}\left(\prod_{i=1}^{K}\left(1-2s(\gamma_i e_i)^{-m_i}\right)\right)d\phi\right]. \quad (12)$$

3.2.2. M-PSK. Since fading parameters m_i and $2m_i$ are integers, P_s for M-PSK modulation can be obtained using (9), and the resultant expression is

$$P_s = \frac{1}{\pi}\int_o^{(M-1)(\pi/M)}\left(\prod_{i=1}^{K}\left(1-2s(\gamma_i e_i)^{-m_i}\right)\right)d\phi. \quad (13)$$

4. Effective Transport Capacity

In the preceding sections, the analysis of dispersed spectrum cognitive radio network by obtaining the error probabilities for different scenarios and the MGF of the dispersed spectrum CR system over Nakagami-m channel is provided. Implementation of dispersed spectrum CR concept in practical wireless networks is of great interest. Therefore, in this section, we considered ad hoc type network for an application of dispersed spectrum CR discussed in the previous sections. The effective transport capacity performance analysis of conventional ad hoc wireless networks considering 2D node distribution is conducted in [14]. In the current section, this analysis is extended to ad hoc dispersed spectrum cognitive radio networks [3], where the nodes are distributed in 3D and they are communicated using the dispersed spectrum cognitive radio systems. In order to derive the effective transport capacity for the ad hoc dispersed spectrum cognitive radio networks, the following network communication system model is employed [14–16].

(i) Each node transmits a fixed power of P_t, and the multihop routes between a source and destination is established by a sequence of minimum length links. Moreover, no node can share more than one route.

(ii) If a node needs to communicate with another node, a multihop route is first reserved and only then the packets can be transmitted without looking at the status of the channel which is based on a MAC protocol for INI: reserve and go (RESGO) [14]. Packet generation, with each packet having a fixed length of D bits, is given by a Poisson process with parameter λ (packets/second).

(iii) The INI experienced by the nodes in the network is mainly dependent on the node distribution and the MAC protocol.

(iv) The condition $\lambda D \leq R_b$, where R_b is transmission data rate of the nodes, needs to be satisfied for network communications.

4.1. Average Number of Hops. In the 3D node configuration, there are W nodes, and each node is placed uniformly at the center of a cubic grid in a spherical volume V that can be defined as

$$V \approx W d_l^3, \quad (14)$$

where d_l is the length of cube that a node is centered in. From (14), it can be shown that two neighboring nodes are at distance d_l which is defined as

$$d_l \approx \left(\frac{1}{\rho_s}\right)^{1/3}, \quad (15)$$

where $\rho_s = W/V(\text{unit}: m^{-3})$ is the node volume density.

The maximum number of hops ($n_h^{\max}$) needs to be determined first in order to derive the expression for average number of hops ($\overline{n}_h$). The deviation from a straight line between the source and destination nodes is limited by assuming that the source and destination nodes lie at opposite ends of a diameter over a spherical surface, and a large number of nodes in the network volume are simulated [14]. It follows that $n_h^{\max}$ distribution can be defined for 3D configuration as

$$n_h^{\max} = \left\lfloor \frac{d_s}{d_l} \right\rfloor = \left\lfloor 2\left(\frac{3W}{4\pi}\right)^{1/3} \right\rfloor, \quad (16)$$

where d_s is the diameter of sphere and $\lfloor\ \rfloor$ represents the integer value closest to the argument.

Since the number of hops is assumed to have a uniform distribution, the probability density function (PDF) can be defined as

$$P_{n_h}(x) = \begin{cases} \dfrac{1}{n_h^{\max}}, & 0 < x < n_h^{\max}, \\ 0, & x = \text{otherwise}, \end{cases} \quad (17)$$

therefore,

$$\overline{n}_h = \int_o^{n_h^{\max}} \frac{1}{n_h^{\max}} x dx = \frac{n_h^{\max}}{2}, \quad (18)$$

which agrees with the result in [14]. The average number of hops for 3D configuration can therefore be obtained as

$$\overline{n}_h = \left\lfloor \left(\frac{3W}{4\pi}\right)^{1/3} \right\rfloor. \quad (19)$$

The total effective transport capacity C_T is the summation of effective transport capacity for each route, and since the routes are disjointed, the C_T is defined as [16]

$$C_T = \lambda L \overline{n}_{\text{sh}} d_l N_{\text{ar}}, \quad (20)$$

where N_{ar} is the number of disjoint routes and $\overline{n}_{\text{sh}}$ is the average number of sustainable hops [16] which is defined as

$$\overline{n}_{\text{sh}} = \min\{n_{\text{sh}}^{\max}, \overline{n}_h\} = \min\left\{\left\lfloor \frac{\ln(1-P_e^{\max})}{\ln(1-P_e^L)} \right\rfloor, \overline{n_h}\right\}, \tag{21}$$

where P_e^L and $p_e^{\max}$ are the bit error rate at the end of a single link and the maximum P_e can be tolerated to receive the data, respectively. The average P_e at the end of a multihop route can therefore be expressed as [15]

$$\overline{P_e} = P_e^{\overline{n}_h} = 1 - (1-P_e)^{\overline{n}_h}. \tag{22}$$

According to (8), P_e is function of MGF, and the MGF of the dispersed spectrum CR system over Nakagami-m channel is given in (7) which is defined as the Laplace transform of the PDF of the SNR [19]. Let the SNR at the end of a single link in the case of conventional single band spectrum utilization be $\gamma_{L,\text{Tot}}$. In addition, let us assume that there exists INI between the nodes, then $\gamma_{L,\text{Tot}}$ can be expressed as [16]

$$\gamma_{L,\text{Tot}} = \alpha^2\left(\frac{CP_t d_l^{-2}}{FK_bT_0R_b + P_{\text{INI}}\eta}\right), \tag{23}$$

where P_t is the transmitted power from each node, F is the noise figure and K_b is the Boltzmann's constant ($K_b = 1.38 \times 10^{-}23$ J/K), T_o is the room temperature ($T_o \approx 300$ K), α is the fading envelope, $\eta = R_b/B_T$ b/s/Hz is the spectral efficiency (where B_T is the transmission bandwidth), P_{INI} is the INI power, and C can be expressed as

$$C = \frac{G_tG_rc^2}{(4\pi)^2 f_l f_c^2}, \tag{24}$$

where G_t and G_r are the transmitter and receiver antenna gains, f_c is the carrier frequency, c is the speed of light, and f_l is a loss factor. From (6) and (23), $\gamma_{L,\text{Tot}}$ for the dispersed spectrum cognitive radio networks can be expressed as

$$\gamma_{L,\text{Tot}} = \sum_{i=1}^{K}\kappa_i\alpha^2\left(\frac{CP_t dl^{-2}}{FK_bT_0R_b + P_{\text{INI}}\eta}\right). \tag{25}$$

Assuming that the destination node is in the center, we try to calculate all the interference powers transmitting from all nodes by clustering the nodes into groups in order to find out the general formula for P_{INI}.

In the xth order tier of the 3D distribution, there are the following.

(i) The interference power at the destination node received from one of six nodes, at a distance xd_l, is $CP_t/(d_lx)^2$.

(ii) The interference power at the destination node received from one of eight nodes, at a distance $x\sqrt{3}d_l$, is $CP_t/(\sqrt{3}d_lx)^2$.

(iii) The interference power at the destination node received from one of twelve nodes, at a distance $x\sqrt{2}d_l$, is $CP_t/(\sqrt{2}d_lx)^2$.

(iv) The interference power at the destination node received from one of twenty nodes, at a distance $\sqrt{x^2+y^2}d_l$, where $y = 1,\ldots,x-1$, and $x \geq 2$, is $CP_t/(d_l^2(x^2+y^2))$.

(v) The interference power at the destination node received from one of twenty nodes, at a distance $\sqrt{2x^2+y^2}d_l$, is $CP_t/(d_l^2(2x^2+y^2))$.

(vi) The interference power at the destination node received from one of twenty nodes, at a distance $\sqrt{x^2+y^2+z^2}d_l$, where $z = 1,2,\ldots,x-1$, $x \geq 2$, is $CP_t/(d_l^2(x^2+y^2+z^2))$.

A maximum W and tier order $x_{\max}$ exist since the number of nodes in the network is finite. Therefore,

$$\begin{aligned} W &\approx \sum_{x=1}^{x_{\max}}(2x+1)^3 - (2(x-1)+1))^3 \\ &\approx \sum_{x=1}^{x_{\max}}24x^2 + 2 = 24\frac{x_{\max}(x_{\max}+1)(2x_{\max}+1)}{6} + 2x_{\max}. \end{aligned} \tag{26}$$

For sufficiently large values of W, (26) leads to $x_{\max} \approx \lfloor W^{1/3}/2 \rfloor$. The probability of a single bit in the packet interfered by any node in the network is defined in [14, 16] as $1 - \exp(-\lambda D/R_b)$ which means that the overall interference power P_{INI} using RESGO MAC protocol can be expressed as [14]

$$P_{\text{INI}}^{\text{RESGO}} = CP_t\rho_s^{2/3}\left(1 - e^{-\lambda D/R_b}\right) \times (\Delta_1 + \Delta_2 + \Delta_3 - 1), \tag{27}$$

where

$$\begin{aligned} \Delta_1 &= \sum_{x=1}^{W^{1/3}/2}\frac{44}{3x^2}, \\ \Delta_2 &= \sum_{x=2}^{W^{1/3}/2}\sum_{y=1}^{x-1}\left(\frac{24}{2x^2+y^2} + \frac{24}{x^2+y^2}\right), \\ \Delta_3 &= \sum_{x=2}^{W^{1/3}/2}\sum_{y=1}^{x-1}\sum_{z=1}^{x-1}\left(\frac{24}{x^2+y^2+z^2}\right). \end{aligned} \tag{28}$$

5. Numerical Results

In this section, numerical results are provided to verify the theoretical analysis. Figure 3 illustrates the effect of frequency diversity order on the average symbol error probability performance of the dispersed spectrum cognitive radio systems. The results are obtained over independent Nakagami-m fading channels considering 16-QAM modulation scheme and the same bandwidth for the frequency diversity bands. The performance of the conventional single band system ($K = 1$) is provided for the sake of comparison. In comparison to the conventional single band system, at $P_s = 10^{-2}$, the dispersed spectrum cognitive radio systems with two

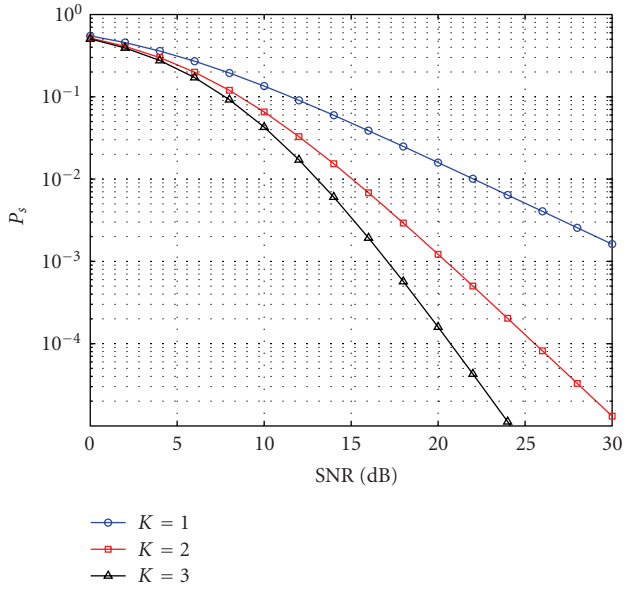

Figure 3: Average symbol error probability versus average SNR per bit for 16-QAM signals with different K values and independent Nakagami-m fading channel ($m = 1$).

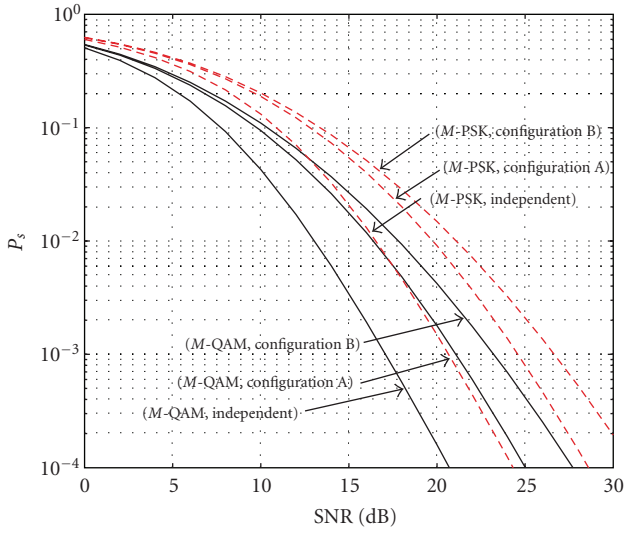

Figure 4: Average symbol error probability versus average SNR per bit for M-QAM and M-PSK signals ($M = 16$) with $K = 3$, Nakagami-m fading channel ($m = 1$) for both independent and dependent channels cases.

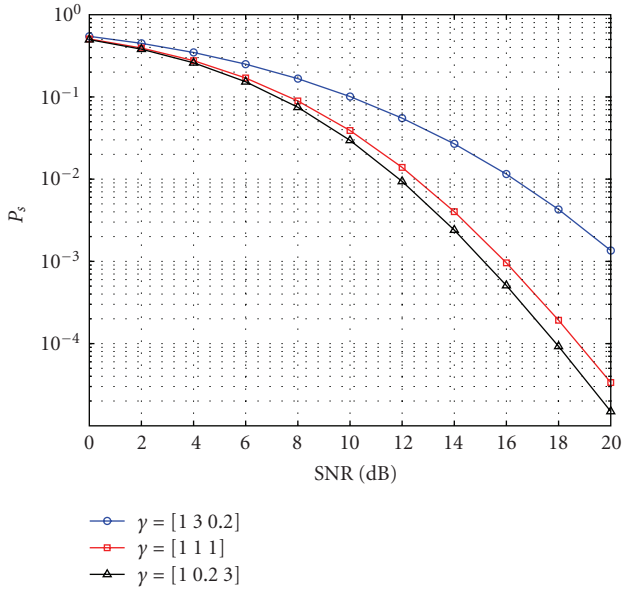

Figure 5: Average symbol error probability versus average SNR per bit for 16-QAM signals with different SNR values at each diversity branch, $m = 1, 0.5, 3$ for $K = 1, 2, 3$, respectively.

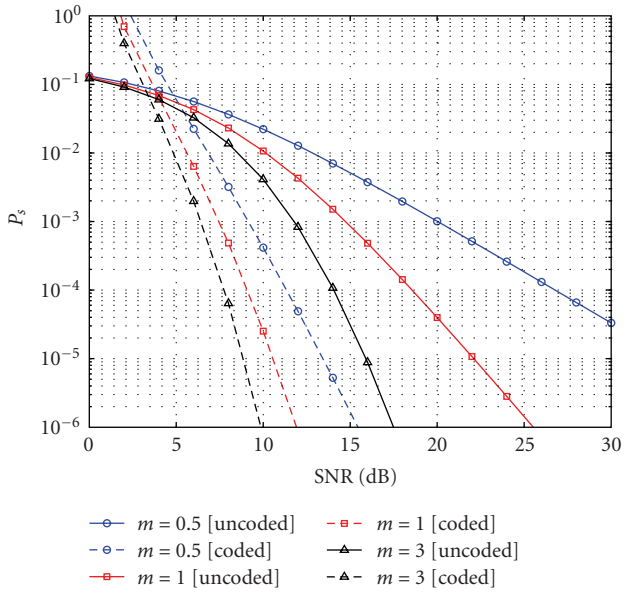

Figure 6: Average symbol error probability versus average SNR per bit for 16-QAM signals with $K = 3$, Nakagami-m fading channel compared with the performance bound for convolutional codes.

frequency diversity bands ($K = 2$) provide SNR gain of 8 dB. An additional 2 dB SNR gain due to the frequency diversity is achieved under the simulation conditions by adding yet another branch ($K = 3$). It is clearly observed that the frequency diversity order is proportional to the performance. In the limiting case, if K goes to infinity the performance converges to the performance of AWGN channel (see the appendix).

Figure 4 presents the performance comparison for the case of using 16-QAM and 16-PSK modulation schemes for independent and dependent cases with equal bandwidth. It is observed that the performance of 16-QAM is better than that of 16-PSK, and this result can be justified since the distance between any points in signal constellation of M-PSK is less than that in M-QAM. This figure shows the performance of the dispersed spectrum cognitive radio systems for the dependent channels case, where Configuration A and Configuration B are considered. It can be seen that the correlation degrades the performance of the system and

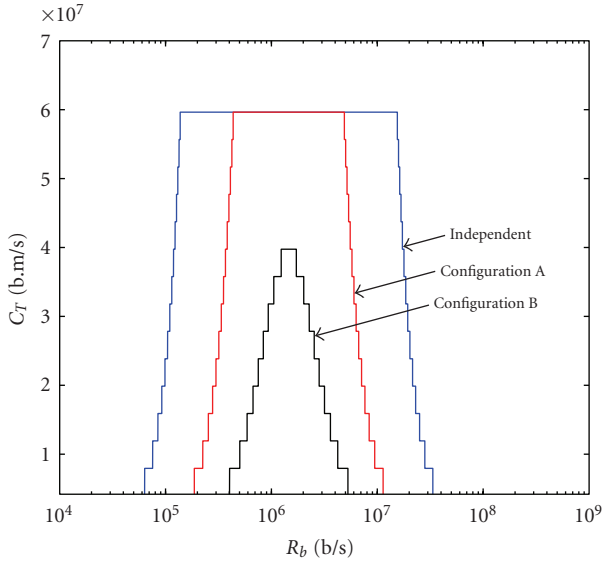

FIGURE 7: C_T versus R_b for 16-QAM modulation with three Nakagami-m fading channels using 3D node distribution ($m = 1$, $K = 3$).

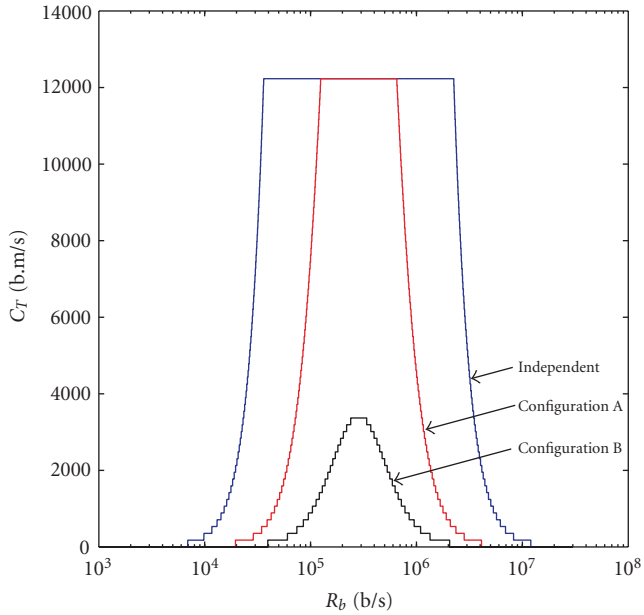

FIGURE 8: C_T versus R_b for 16 QAM modulation with three Nakagami-m fading channels using 2D node distribution ($m = 1, K = 3$).

it can also be noted that Configuration A case performs better than Configuration B case. This is due to the fact that Configuration B has lower correlation coefficients than those of Configuration A.

In Figure 5, the effects of frequency diversity branches with different SNR values on the symbol error probability performance are shown. (The SNR value for each frequency diversity branch is given by γ_r (e.g., $\gamma_r = [\gamma_1 \gamma_2 \gamma_3]$).) These different SNR values for the diversity bands are assigned relative to the SNR value of the first band; for instance, for the SNR values of $\gamma_r = [\gamma_1 \quad \gamma_2 \quad \gamma_3] = [1 \quad 3 \quad 0.2]$, the SNR value of second band is three times the first band. It can be noted that the system performs better if the branch with the lowest fading severity has the highest SNR, since the symbol error probability mainly depends on the SNR proportionally, and fading parameter m.

The effects of coding on the performance of the system are also investigated. The convolutional coding with $(2, 1, 3)$ code and $g(0) = (1\ 1\ 0\ 1)$, $g(1) = (1\ 1\ 1\ 1)$ generator matrices are considered. The bound for error probability in [24] is extended for our system and it is used as performance metric during the simulations. Finally, Nakagami-m fading channel along with 16-QAM modulation is assumed. The result is plotted in Figure 6 which shows the effects of coding on the performance and it can be clearly seen that the performance is improved due to coding gain.

The results in Figures 7 and 8 are obtained using the following network simulation parameters: $G_t = G_r = 1$, $f_l = 1.56\,\text{dB}$, $F = 6\,\text{dB}$, $V = 1 \times 10^6\,\text{m}^3$, $\lambda D = 0.1\,b/s$, $P_t = 60\,\mu W$, and $W = 15000$. In order for the numerical results to be comparable to the results in [14], we choose the value of $m = 1$ for Nakagami-m fading channels, which represents Rayleigh fading channels. The effects of 3D node distribution on the effective transport capacity of ad hoc dispersed spectrum cognitive radio networks are investigated through computer simulations considering $K = 3$ dispersed channels between two nodes, and the results are shown in Figure 7. In ad hoc model the dependency of K channels is assumed to be the same as dependent channels case in Section 3.2. This figure represents the relationship between the bit rate and the effective transport capacity considering 3D node distribution. It is shown that at low and high R_b values, the effective transport capacity is low. However, at intermediate values, the effective transport capacity is saturated. This is due to the fact that the average sustainable number of hops is defined as the minimum between the maximum number of sustainable hops and the average number of hops per route. Full connectivity will not be sustained until reaching the average number of hops. Having reached the average number of hops, full connectivity will be sustained until the number of hops is greater than the threshold value as defined by an acceptable BER, since a low SNR value is produced by low and high R_b values. It can be seen that the correlation between fading channels degrades the performance of the system and it can also be noted that Configuration A case performs better than Configuration B case.

It is known that the deployment of an ad hoc network is generally considered as two dimensions (2D). Nonetheless, because of reducing dimensionality, the deployment of the nodes in a 3D scenario are sparser than in a 2D scenario, which leads to decrease of the internodes interference, thus increasing the effective transport capacity of the system. This can be observed by comparing Figures 7 and 8.

In addition, the 3D topology of dispersed spectrum cognitive radio ad hoc network can be considered in some real applications such as sensor network in underwater, in which the nodes may be distributed in 3D [13]. The 3D topology is more suitable to detect and observe the phenomena in

the three dimensional space that cannot be observed with 2D topology [25].

6. Conclusion

In this paper, the performance analysis of dispersed spectrum cognitive radio systems is conducted considering the effects of fading, number of dispersed bands, modulation, and coding. Average symbol error probability is derived when each band undergoes independent and dependent Nakagami-m fading channels. Furthermore, the average symbol error probability for both cases is extended to take the modulation effects into account. In addition, the effects of coding on symbol error probability performance are studied through computer simulations. We also study the effects of the 3D node distribution along with INI on the effective transport capacity of ad hoc dispersed spectrum cognitive radio networks. The effective transport capacity expressions are derived over fading channels considering M-QAM modulation scheme. Numerical results are presented to study the effects of fading, number of dispersed bands, modulation, and coding on the performance of dispersed spectrum cognitive radio systems. The results show that the effects of fading, number of dispersed bands, modulation, and coding on the average symbol error probability of dispersed spectrum cognitive radio systems is significant. According to the results, the effective transport capacity is saturated for intermediate bit rate values. Additionally, it is concluded that the correlation between fading channels highly affects the effective transport capacity. Note that this work can be extended to the case where the number of available bands change randomly at every spectrum sensing cycle, which is considered as a future work.

Appendix

The MGF of Nakagami-m fading channels of dispersed spectrum sharing system with K available bands is given by

$$\mu(s) = \left(\frac{1}{1 - s\gamma/mK}\right)^{mK}. \tag{A.1}$$

For $K = \infty$ (or $m = \infty$), we obtain the form of type 1^{∞}. The solution is given by introducing a dependant variable

$$y = \left(\frac{1}{1 - s\gamma/mK}\right)^{mK}, \tag{A.2}$$

and taking the natural logarithm of both sides:

$$\ln(y) = mK \ln\left(\frac{1}{1 - s\gamma/mK}\right) = \frac{\ln(1/(1 - s\gamma/mK))}{1/mK}. \tag{A.3}$$

The limit $\lim_{K,m\to\infty} \ln(y)$ is an indeterminate form of type 0/0; by using L'Hôpital's rule we obtain

$$\lim_{K,m\to\infty} \ln(y) = \frac{\ln(1/(1 - s\gamma/mK))}{1/mK} = s\gamma. \tag{A.4}$$

Since $\ln(y) \to s\gamma$ as $m \to \infty$ or $K \to \infty$, it follows from the continuity of the natural exponential function that $e^{\ln(y)} \to e^{s\gamma}$ or, equivalently, $y \to e^{s\gamma}$ as $K \to \infty$ (or $m \to \infty$).

Therefore,

$$\lim_{K,m\to\infty} \left(\frac{1}{(1 - s\gamma/mK)}\right)^{mK} = e^{s\gamma}. \tag{A.5}$$

Since the MGF of the Gaussian distribution with zero variance is given by

$$\mu_g(s) = e^{s\gamma}, \tag{A.6}$$

we conclude that, when $K \to \infty$, the channel converges to an AWGN channel under the assumption independent channel samples.

Acknowledgment

This paper was supported by Qatar National Research Fund (QNRF) under Grant NPRP 08-152-2-043.

References

[1] J. Mitola and G. Q. Maguire, "Cognitive radio: making software radios more personal," *IEEE Personal Communications*, vol. 6, no. 4, pp. 13–18, 1999.

[2] S. Ekin, F. Yilmaz, H. Celebi, K. A. Qaraqe, M. Alouini, and E. Serpedin, "Capacity limits of spectrum-sharing systems over hyper-fading channels," *Wireless Communications and Mobile Computing*. In press.

[3] S. Gezici, H. Celebi, H. V. Poor, and H. Arslan, "Fundamental limits on time delay estimation in dispersed spectrum cognitive radio systems," *IEEE Transactions on Wireless Communications*, vol. 8, no. 1, pp. 78–83, 2009.

[4] S. Gezici, H. Celebi, H. Arslan, and H. V. Poor, "Theoretical limits on time delay estimation for ultra-wideband cognitive radios," in *Proceedings of the IEEE International Conference on Ultra-Wideband (ICUWB '08)*, vol. 2, pp. 177–180, September 2008.

[5] H. Celebi, K. A. Qaraqe, and H. Arslan, "Performance comparison of time delay estimation for whole and dispersed spectrum utilization in cognitive radio systems," in *Proceedings of the 4th International Conference on Cognitive Radio Oriented Wireless Networks and Communications (CROWNCOM '09)*, pp. 1–6, June 2009.

[6] F. Kocak, H. Celebi, S. Gezici, K. A. Qaraqe, H. Arslan, and H. V. Poor, "Time delay estimation in cognitive radio systems," in *Proceedings of the 3rd IEEE International Workshop on Computational Advances in Multi-Sensor Adaptive Processing (CAMSAP '09)*, pp. 400–403, 2009.

[7] F. Kocak, H. Celebi, S. Gezici, K. A. Qaraqe, H. Arslan, and H. V. Poor, "Time-delay estimation in dispersed spectrum cognitive radio systems," *EURASIP Journal on Advances in Signal Processing*, vol. 2010, Article ID 675959, 2010.

[8] T. Chen, H. Zhang, G. M. Maggio, and I. Chlamtac, "Topology management in CogMesh: a cluster-based cognitive radio mesh network," in *Proceedings of the IEEE International Conference on Communications (ICC '07)*, pp. 6516–6521, Citeseer, 2007.

[9] P. Mähönen, M. Petrova, and J. Riihijärvi, "Applications of topology information for cognitive radios and networks," in *Proceedings of the 2nd IEEE International Symposium on New Frontiers in Dynamic Spectrum Access Networks (DySPAN '07)*, pp. 103–114, April 2007.

[10] A. Chiganmi, K. Sarac, and R. Prakash, "Variable power broadcasting in ad hoc networks," in *Proceedings of the IEEE International Conference on Communications (ICC '06)*, Citeseer, Istanbul, Turkey, 2006.

[11] J. Hoydis, M. Petrova, and P. Mähönen, "Effects of topology on local throughput-capacity of ad hoc networks," in *Proceedings of the 19th IEEE International Symposium on Personal, Indoor and Mobile Radio Communications (PIMRC '08)*, pp. 1–5, September 2008.

[12] R. W. Thomas, R. S. Komali, A. B. MacKenzie, and L. A. DaSilva, "Joint power and channel minimization in topology control: a cognitive network approach," in *Proceedings of the IEEE International Conference on Communications (ICC '07)*, pp. 6538–6544, June 2007.

[13] D. Pompili, T. Melodia, and I. F. Akyildiz, "Three-dimensional and two-dimensional deployment analysis for underwater acoustic sensor networks," *Ad Hoc Networks*, vol. 7, no. 4, pp. 778–790, 2009.

[14] G. Ferrari, B. Baruffini, and O. Tonguz, "Spectral efficiency-connectivity tradeoff in ad hoc wireless network," in *Proceedings of the International Symposium on Information Theory and Its Applications (ISITA '04)*, Parma, Italy, October 2004.

[15] G. Ferrari and O. K. Tonguz, "MAC protocols and transport capacity in ad hoc wireless networks: Aloha versus PR-CSMA," in *Proceedings of the IEEE Military Communications Conference (MILCOM '03)*, pp. 1311–1318, Boston, Mass, USA, October 2003.

[16] O. Tonguz and G. Ferrari, *Ad Hoc Wireless Networks: A Communication Theoretic Perspective*, John Wiley & Sons, New York, NY, USA, 2006.

[17] K. A. Qaraqe, M. Mohammad, H. Celebi, and A. El-Saigh, "The impacts of node distribution on the effective transport capacity of ad hoc dispersed spectrum cognitive radio networks," in *Proceedings of the 17th International Conference on Telecommunications (ICT '10)*, pp. 122–127, Doha, Qatar, October 2010.

[18] H. Celebi, K. A. Qaraqe, and H. Arslan, "Performance analysis of TOA range accuracy adaptation for cognitive radio systems," in *Proceedings of the 70th IEEE Vehicular Technology Conference Fall (VTC '09)*, Anchorage, Alaska, USA, September 2009.

[19] A. Goldsmith, *Wireless Communciations*, Cambridge University Press, Cambridge, UK, 2005.

[20] W. C. Y. Lee, *Mobile Communications Design Fundamentals*, John Wiley & Sons, New York, NY, USA, 1993.

[21] Q. T. Zhang, "Exact analysis of postdetection combining for DPSK and NFSK systems over arbitrarily correlated nakagami channels," *IEEE Transactions on Communications*, vol. 46, no. 11, pp. 1459–1467, 1998.

[22] M. Nakagami, "The m distribution—a general formula for intensity distribution of rapid fading," in *Statistical Methods in Radio Wave Propagation*, W. G. Hoffman, Ed., pp. 3–66, Pergamon, New York, NY, USA, 1960.

[23] I. Ghareeb, "Noncoherent MT-MFSK signals with diversity reception in arbitrarily correlated and unbalanced Nakagami-*m* fading channels," *IEEE Journal on Selected Areas in Communications*, vol. 23, no. 9, pp. 1839–1850, 2005.

[24] S. Lin and D. Castello, *Error Control Coding*, Pearson, Prentice Hall, Upper Saddle River, NJ, USA, 2nd edition, 1963.

[25] R. Tiwari, T. Dinh, and M. Thai, *On Approximation Algorithms for Interference-Aware Broadcast Scheduling in 2D and 3D Wireless Sensor Networks*, Springer Wireless Algorithms, Systems, and Applications, Springer, New York, NY, USA, 2009.